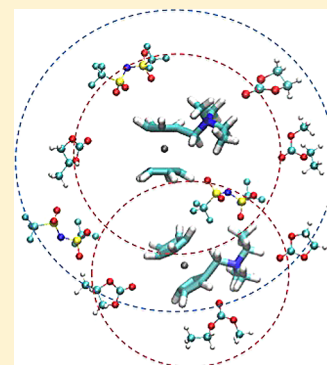


Preferential Solvation of an Asymmetric Redox Molecule

Kee Sung Han,^{†,§} Nav Nidhi Rajput,^{‡,§} M. Vijayakumar,^{*,†,§} Xiaoliang Wei,^{†,§} Wei Wang,[†] Jianzhi Hu,^{†,§} Kristin A. Persson,^{‡,§,⊥} and Karl T. Mueller^{*,†,§}[†]Pacific Northwest National Laboratory, Richland, Washington 99352, United States[‡]Lawrence Berkeley National Laboratory, Berkeley, California 94720, United States[§]Joint Center for Energy Storage Research (JCESR), Lemont, Illinois 60439, United States[⊥]Department of Materials Science & Engineering, University of California, Berkeley, California 94720, United States

Supporting Information

ABSTRACT: The fundamental correlations between solubility and solvation structure for the electrolyte system comprising *N*-(ferrocenylmethyl)-*N,N*-dimethyl-*N*-ethylammonium bistrifluoromethylsulfonimide (Fc1N112-TFSI) dissolved in a ternary carbonate solvent mixture is analyzed using combined NMR relaxation and computational methods. Probing the evolution of the solvent–solvent, ion–solvent and ion–ion interactions with an increase in solute concentration provides a molecular level understanding of the solubility limit of the Fc1N112-TFSI system. An increase in solute concentration leads to pronounced Fc1N112-TFSI contact-ion pair formation by diminishing solvent–solvent and ion–solvent type interactions. At the solubility limit, the precipitation of solute is initiated through agglomeration of contact-ion pairs due to overlapping solvation shells.

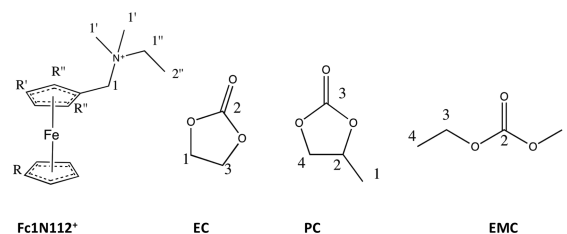


INTRODUCTION

Functional properties of an electrolyte such as solubility, viscosity, and ionic conductivity primarily depend on the intricate interaction between solute and solvent molecules, which is commonly referred to as solvation phenomena.^{1,2} Although solvation phenomena involving single atom solutes in neat solvents are reasonably well understood, a realistic electrolyte system containing polyatomic solutes with asymmetric structures and mixtures of complex solvents presents additional challenges.^{3,4} In particular, the asymmetric charge distribution around the polyatomic solutes can facilitate competition between solvent molecules and counter-anions to solvate specific regions of the solute, causing preferential solvation. The subtle interplay of such a highly correlated and dynamic interaction between solute and solvent typically emerges as the functional properties of modern electrolytes. For example, the ferrocene-derived solute *N*-(ferrocenylmethyl)-*N,N*-dimethyl-*N*-ethylammonium cation (Fc1N112⁺) with bistrifluoromethylsulfonimide (TFSI⁻) counteranion (see Scheme 1) is about 20 times more soluble than unmodified ferrocene in a ternary solvent mixture comprising propylene carbonate (PC), ethyl methyl carbonate (EMC), and ethylene carbonate (EC).^{5,6} This solvent mixture system is successfully used in nonaqueous redox flow battery technology.^{5,6}

This polyatomic redox active solute dissolved in a solvent mixture offers new opportunities to investigate how preferential solvation dictates the solubility limit of electrolytes. Herein, we demonstrate a correlation of the macroscopic solubility with nano- to mesoscale solvation phenomena, which is an essential

Scheme 1. Molecular Structure and Proton Site Numbering for EC, PC, EMC, and the Fc1N112⁺ Cation



step toward rational design of electrolytes. In particular, the asymmetric structure and charge distribution of the Fc1N112⁺ species when dissolved in a three-component solvent mixture (EC/PC/EMC 4:1:5 by weight) leads to highly correlated interactions including solvent–solvent, ion–ion and solvent–ion interactions. The challenge is that these correlated interactions can span over wide spatial (up to a few nanometers) and temporal (from picoseconds to a few seconds) scales. To access the critical spatial and temporal ranges of this preferential solvation, we have employed nuclear magnetic resonance (NMR)-based relaxation measurements coupled with classical molecular dynamics (MD) computational methods.

Received: September 14, 2016

Revised: November 9, 2016

Published: November 14, 2016

EXPERIMENTAL METHODS

Sample Preparations. To improve low ferrocene solubility in the electrolyte (0.2 M in the EC/PC/EMC solvent studied here), a ferrocene-based ionic liquid compound (Fc1N112-TFSI, shown in Scheme 1) was prepared. Starting from (dimethylaminomethyl)ferrocene (Fc1N11), the Fc1N112-TFSI was synthesized via a nucleophilic substitution reaction utilizing bromoethane to yield the intermediate compound, dimethyl ethyl ferrocenylmethylammonium bromide (Fc1N112-Br), followed by anion exchange with TFSI⁻ to afford the Fc1N112-TFSI at an overall two-step yield of 91%. The experimental details of the preparation can be found elsewhere.⁵ By virtue of the structural modification, the resulting Fc1N112-TFSI shows a dramatically enhanced solubility (up to 1.7 M) in the EC/PC/EMC solvent system.⁵

NMR Measurements. To analyze the solvation phenomena through molecular reorientational dynamics, the rotational correlation times (τ_c) of different regions of Fc1N112⁺ and solvent molecules (through each resolved ¹H site, Figure S1) were calculated from the proton (¹H) spin–lattice relaxation time (T_1). The ¹H T_1 of Fc1N112⁺ cation and solvent molecules, EC, PC, and EMC (Scheme 1) in neat and Fc1N112-TFSI-dissolved PC, EMC, and EC/PC/EMC were measured with the inversion recovery (180- τ -90-acquisition sequence) at a Larmor frequency of 599.82 MHz in the temperature range from 193 to ~373 K using a 600 MHz NMR spectrometer (Agilent, USA) equipped with a 5 mm liquid NMR probe (Doty Scientific, USA). The reorientational correlation times, τ_c , of each resolved site for Fc1N112⁺ cation, EC, PC and EMC were calculated from measured ¹H T_1 values using the Bloembergen-Purcell-Pound (BPP) equation (see Supporting Information (SI)). Errors associated with measurement and data analysis (curve fitting) are less than 5% for all the reported values.

Classical Molecular Dynamics Simulations. Classical molecular dynamics (MD) simulations were performed using the GROMACS MD simulation package version 4.5.3.⁷ The molecules are initially packed randomly in a cubic box of size 50 × 50 × 50 Å³ that is periodic in the XYZ direction using PACKMOL.⁸ The initial configuration is minimized in two steps, first using steepest descent employing a convergence criterion of 1000 kcal/mol-Å followed by a conjugated-gradient energy with convergence criterion of 10 kcal/mol-Å. The systems were then equilibrated in the isothermal–isobaric ensemble (constant NPT) using the Berendsen barostat to maintain the pressure of 1 bar with a time constant of 2 ps for 2 ns. After obtaining the correct density from the NPT ensemble, all systems were melted at 400 K for 2 ns and subsequently annealed from 400 to 298 K in three steps of 2 ns each to ensure that the molecules are not trapped in metastable states. The production runs of 10 ns were then obtained in the canonical ensemble (NVT) using an improved velocity-rescaling algorithm proposed by Parrinello et al.⁹ with a time constant of 0.1 ps over the temperature range of 273 to 323 K. The force field and the remainder of the simulation procedure used in this work are identical to those described in detail in our previous paper.¹⁰

RESULTS AND DISCUSSION

Identifying the solvent specific ion–solvent interaction is the first step in deciphering preferential solvation in different solvent mixtures. It is expected that the solvent molecules will

have poor interaction with the weakly coordinating TFSI⁻ anions due to their relatively smaller Lewis basicities. This aspect is supported by the weak interaction between TFSI⁻ anion and solvent molecules observed in our MD analysis (Figure S2). Therefore, we focus on the preferential solvation around the Fc1N112⁺ cations comprising solvent molecules and TFSI⁻ anions as they control the functional properties of the electrolyte. Initially, we analyzed the proton T_1 relaxation time behavior of the solvent molecules in a neat solvent system (i.e., pure PC or EMC solutions only, as EC is a solid at room temperature) and subsequently introduced a low concentration (0.25 M) of Fc1N112-TFSI redox molecules.

Figure 1 compares and contrasts the temperature-dependent T_1 relaxation behavior of the neat solvent and molecules within

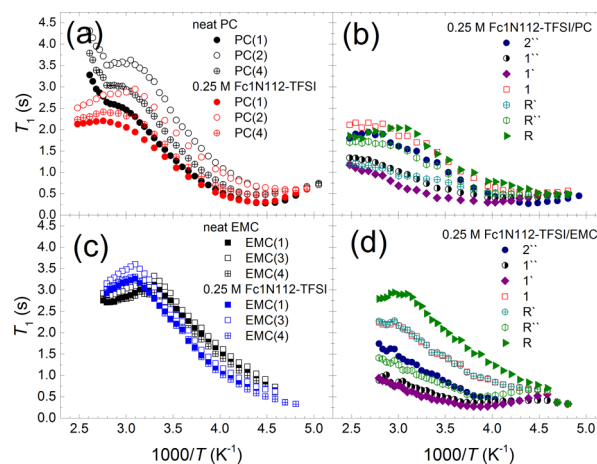


Figure 1. Variable temperature proton (¹H) NMR spin–lattice relaxation time (T_1) values for the solvent molecules and Fc1N112⁺ cations in neat solvents and 0.25 M Fc1N112-TFSI dissolved in PC (panels a and b) and in EMC (panels c and d). For specific proton site labeling within Fc1N112⁺ and solvent molecules, see Scheme 1.

the 0.25 M solutions of Fc1N112-TFSI in the single solvent systems. Examining the evolution of the solvent relaxation behavior that occurs upon introduction of Fc1N112⁺ provides the necessary baseline description of the preferential interaction of each solvent alone around the Fc1N112⁺ cations. For example, the significantly reduced T_1 values (see Figure 1a) of the protons within PC molecules in the high temperature region when compared to the values of those in pure PC solution indicates that the PC molecules are primarily located near the paramagnetic center (i.e., Fe²⁺) in cyclopentadienyl rings of the Fc1N112⁺ cations. On the other hand, similar T_1 values (see Figure 1c) for protons in the EMC molecules in the solution relative to their values in the neat solvent indicates the absence of a paramagnetic relaxation effect, and hence their preferred interaction is with the alkylammonium ionic chains of Fc1N112⁺ cations. Such a site-specific ion–solvent interaction can also be observed, through the intramolecular dynamics of Fc1N112⁺ cations. In particular, the anisotropic dynamics of Fc1N112⁺ arising from its asymmetric structure and charge distribution will further be modulated by interactions of solvent molecules enveloping the preferential site. The ¹H nuclei in both cyclopentadienyl rings (i.e., R, R' and R'' sites of Fc1N112⁺) register relatively shorter T_1 values in PC solvent than those in EMC solvent, while the T_1 values for the ionic chain nuclei (i.e., 1', 1'' and 2'' sites of Fc1N112⁺) are relatively shorter in EMC solvent than those in PC (see Figure 1b,d).

Such a solvent-specific dampening of relaxation (i.e., shorter T_1) indicates that PC molecules are strongly interacting with cyclopentadienyl rings, whereas the EMC solvent has relatively stronger interaction with the ionic chain. To further analyze the solvation structure through reorientational dynamics, the rotational correlation times (τ_C) of different regions of Fc1N112⁺ and solvent molecules (through each resolved ¹H site) were calculated using the Bloembergen–Purcell–Pound (BPP) equation (see SI).¹¹ We confirmed the validity of BPP theory in these solutions by comparison of the τ_C values for the neat PC solvent obtained by ¹H T_1 and other techniques (see SI, Figure S3). The average ratio between the reorientation rate (τ_C^{-1}) of untethered ring (R) sites to those from the tethered ring (R' and R''), i.e., $\Gamma = \tau_C(R)^{-1}/\tau_C(R')^{-1}$, is slightly larger when 0.25 M Fc1N112-TFSI is dissolved in PC ($\Gamma = 1.8$) than in EMC ($\Gamma = 1.5$). This specific solvent modulation of the internal dynamics of Fc1N112⁺ clearly indicates the preferential interaction of the enveloping solvent molecules. MD simulations confirm preferential interaction of PC with the Fe²⁺ center in cyclopentadienyl rings and EMC with the ionic chain (Figure S4), corroborating the NMR-based conclusions.

To obtain higher solubility for the redox molecule studied here, a more complex carbonate solvent mixture system is required, and of course, we cannot presume that the preferential interaction of solutes with competing solvent molecules is independent of solute concentrations or molar composition of more complex solvents. The ¹H T_1 relaxation behaviors of the solvent molecules and Fc1N112⁺ cations at higher solute concentrations (0.85 and 1.7 M) in an EC/PC/EMC solvent mixture are shown in Figure 2. In general, as the

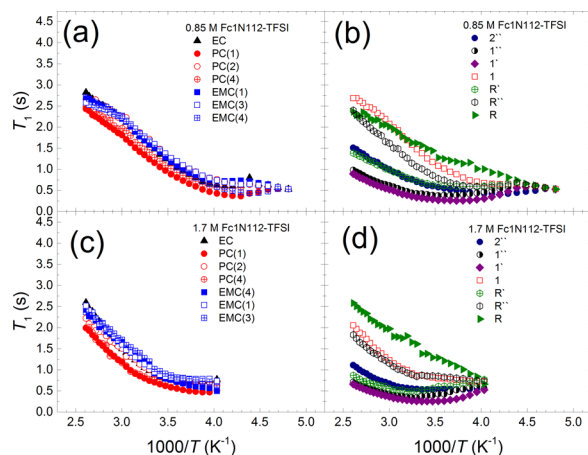


Figure 2. Variable temperature proton (¹H) NMR spin–lattice relaxation time (T_1) values of solvent molecules (EC/PC/EMC) and Fc1N112⁺ cation in 0.85 M (panels a and b) and 1.7 M (panels c and d) solutions.

solute concentration increases, the minima in the ¹H relaxation times ($T_{1, \min}$) of Fc1N112⁺ species and all solvent molecules shift to higher temperature due to slowing down of their reorientational motions. In particular, at the solubility limit (1.7 M) the ¹H T_1 values of Fc1N112⁺ decrease further (except for that of the untethered ring R) and $T_{1, \min}$ displays shifts toward higher temperatures, indicating enhanced ion–solvent interactions and slower reorientational motion, respectively. In addition, the degree of the T_1 curvature at $T_{1, \min}$ (i.e., depth of the $T_{1, \min}$) is inversely proportional to the distance between the observed protons¹² (for example intramolecular interaction

between methyl protons). Therefore, if the measured T_1 values are solely due to the intramolecular interaction, the T_1 curvatures for each site should be the same for all samples, and the T_1 curve should be symmetric at $T_{1, \min}$. However, the observed T_1 curves are not symmetric, and the T_1 curvature of Fc1N112⁺ becomes deeper, while the solvent molecules register shallower curvature with an increase in solute concentration (see Figures 1 and 2). Such pronounced changes in T_1 curvature indicate the evolution of proton–proton mean distances arising from intermolecular rather than the intramolecular homonuclear interactions where the mean distance would remain constant irrespective of Fc-TFSI concentrations.¹³ The proton distance, estimated at the $T_{1, \min}$ using the BPP theory (eq S3), $r_{H-H} \approx 1.82 \pm 0.03$ Å for CH₃ groups for PC(1) and EMC(4) molecules in neat EC/PC/EMC is very close to its theoretical value of 1.78 Å. With increase in solute concentration to 0.85 and 1.7 M, the r_{H-H} distances of these CH₃ groups calculated from $T_{1, \min}$ increase to 2.07 ± 0.04 and 2.20 ± 0.07 Å, respectively, while the r_{H-H} of the site 2'' on the Fc1N112⁺ cation decreases (Figure S5). These variations of r_{H-H} exceed the possible error (<5%) due to the distribution of rotational correlation times resulting from anisotropic molecular motions.¹⁴ Therefore, we hypothesize that the increase of the solute concentration decreases the mean distance between two successive Fc1N112⁺ cations whereas the solvent molecules move apart, which is also supported by our MD analysis (Figure S6).

Importantly, at higher concentrations, this behavior leads to overlapping of Fc1N112⁺ solvation spheres, greatly affecting the solvent–solvent and ion–solvent interactions. Such overlapping solvation shells could lead to the unique solvent reorientational dynamics and intramolecular dynamics of the Fc1N112⁺ cations at higher solute concentrations. The relative degree of reorientational motion for each site of solvent and solute molecules estimated from the position of T_1 minimum (where $\tau_C \approx 0.616/\omega_0$) is shown in Figure 3.

In the neat EC/PC/EMC solvent mixture, the solvent–solvent interaction is exclusive, which results in well-averaged reorientational motion (i.e., similar $T_{1, \min}$) for all solvent molecules due to an eutectic effect (see Figure 3a). With introduction of solute, the solvent reorientational motion slows down significantly. Nevertheless, the solvent reorientational motion is still higher than the overall molecular reorientation motion of Fc1N112⁺ cations for all solute concentrations (see Figure 3b). Thus, with increases in solute concentrations, the stronger ion–ion¹⁵ and ion–solvent interactions become dominant and replace the weaker solvent–solvent interactions, which can be correlated to the increased mean distance between adjacent solvent molecules discussed earlier. In fact, the slower reorientation (i.e., increased τ_C) of solvent molecules with increases in Fc1N112-TFSI concentration also implies a drop in availability of free solvent molecules (i.e., bulk solvent) due to their increased probability to take part in the solvation process. Uninterrupted and stronger ion–solvent interactions effectively screen the overall reorientational dynamics of the solvent molecules through preferential solvation structures. Further analysis of anisotropic reorientational dynamics within Fc1N112⁺ (see Figure 3b and Figure S7) reveals the evolution of preferential ion–solvent interaction with solute concentrations. The reorientation motion of an untethered ring (site R) is relatively faster than the ionically tethered ring and less affected by the Fc1N112-TFSI concentration. The average ratio between the reorientation rates of the two rings at 0.85 M

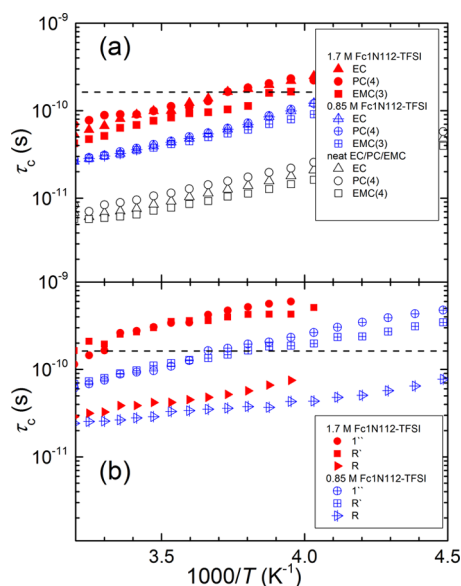


Figure 3. τ_c for (a) solvent molecules EC, PC, and EMC and (b) Fc1N112⁺ cations in neat EC/PC/EMC mixture and 0.85 and 1.7 M Fc1N112-TFSI dissolved in EC/PC/EMC. For specific proton site labeling within Fc1N112⁺ and solvent molecules, see Scheme 1. The dotted lines mark $\tau_c = 0.163$ ns, the τ_c determined by the Larmor frequency of the protons in the NMR experiment performed at 11.4 T ($\omega_0\tau_c \approx 0.616$) at T_1 minima.

concentration is found to be significantly higher ($\Gamma = 2.8$) than within the 0.25 M single solvent systems (*vide infra*). Although the τ_c for the untethered ring (site R) in a saturated solution (1.7 M) is not available, its temperature-dependent T_1 behavior is similar to that found for the 0.85 M system. Hence, assuming the same $\tau_c(R)^{-1}$ as the 0.85 M solution, the ratio for the saturated solution will have an approximate 4-fold increase (i.e., $\Gamma \approx 10$), which is comparable to values reported for acetyl (~ 4) and butyl (~ 7) substituted ferrocene species.¹⁶ This increased anisotropy in intramolecular dynamics indicates that, at higher concentrations, the solvent molecules (except PC) and counteranions are preferentially enveloping the ionic chain and tethered ring site of the Fc1N112⁺ cations, respectively. With an increase in concentration, the untethered ring retains the rotational dynamics, whereas the tethered ring slows down due to preferential ion–solvent and ion–ion interactions. Such asymmetric interaction is further supported by significantly lower reorientational dynamics of solvent molecules at higher solute concentrations (see Figure 3a). This observation also indicates that preferential solvation diminishes solvent–solvent interactions typically observed within the second solvation sphere and bulk solvent system. Hence, at the solubility limit, fewer bulk solvent molecules occupy the second solvation sphere, leading to a highly porous solvation environment for the Fc1N112⁺ cations. Porous solvation represents the missing solvent molecules within a solvation shell due to scarcity at higher solute concentration. This porosity enhances the probability of ion–ion interactions between the Fc1N112⁺ and TFSI[−], leading to contact-ion pair (CIP) formation, which is likely dominant over ion–solvent and solvent–solvent interactions. The CIP represents the ion association in solution, where oppositely charged ions are in contact with each other while maintaining most of their solvation shell.^{17,18} As discussed earlier from $T_{1,\min}$ curvature analysis, at higher concentrations, the mean distance between two successive

Fc1N112⁺ cations decreases, whereas the solvent molecules move apart. Hence, the mean distance between successive CIPs will further decrease to facilitate larger aggregate formation. Such agglomeration of CIPs will initiate the precipitation processes by acting as crystallization seeds that set the solubility limit (≤ 1.7 M) of this electrolyte system. Typically, such cluster formation leads to extended structure formation and subsequent solute precipitation.^{19,20} Such a preferential solvation induced solubility limit can be further analyzed using results from MD simulations.

Figure 4 shows values of the coordination number (CN) of TFSI[−] and solvent molecules with respect to both the ring side

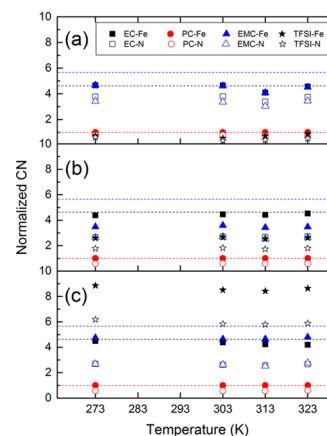


Figure 4. Temperature-dependent coordination numbers (CNs) of TFSI[−] counteranions and solvent molecules with respect to the iron center of cyclopentadienyl rings (solvent/anion-Fe) and nitrogen center of alkylammonium ionic liquid chains (solvent/anion-N) calculated from radial distribution functions obtained from MD simulations as a function of Fc1N112-TFSI concentration: (a) 0.25, (b) 0.85 and (c) 1.7 M. The solvent CNs are normalized with respect to CN (PC-Fe) and specific number concentration in the solvent mixture (i.e., EC/PC/EMC in a 4.637/1/5.667 number ratio) is denoted with the dotted lines black/red/blue, respectively.

and ionic portion of Fc1N112⁺ at different solute concentrations (0.25, 0.85, and 1.7 M) in the 273–323 K temperature interval (see SI). These results illuminate the mesoscale picture of preferential solvation.²¹ The solvent and anion CNs with Fc1N112⁺ are identified based on their interaction with either the Fe²⁺ center at the cyclopentadienyl rings (i.e., solvent-Fe) or the N⁺ center of the ionic chain (i.e., solvent-N) and subsequently normalized based on their respective number ratio within the EC/PC/EMC mixture. This representation tracks the solvent/anion position in the solvation structure over various salt concentrations as well as temperature regions. The cation–solvent CN remains the same, whereas the cation–anion CN increases with an increase in salt concentration, indicating that the average distance between adjacent solvent molecules increases, resulting in a decrease in solvent–solvent CN (see Figure S8) while the ionic solutes (i.e., Fc1N112⁺ and TFSI[−]) are positioned closer. Despite the rise of CN between counterions (i.e., contact-ion pair formation), the strength of the interactions between the ring-side of Fc1N112⁺ and TFSI[−] is relatively weaker than the solvent–Fc1N112⁺ pairings due to possible effects of steric hindrance (see Figure S9). Even under contact-ion pair formation, the relatively weaker attraction between counterions can lead to fairly independent dynamics of Fc1N112⁺ and TFSI[−] as reported in our previous diffusional

measurements.¹⁰ To further evaluate the ion–ion interaction strength under CIP formation, we analyzed the average bond distances between Fc1N112⁺ and TFSI[−] through the examination of the MD-derived radial distribution functions (RDFs). Figure 5a displays the RDF analysis of TFSI[−]

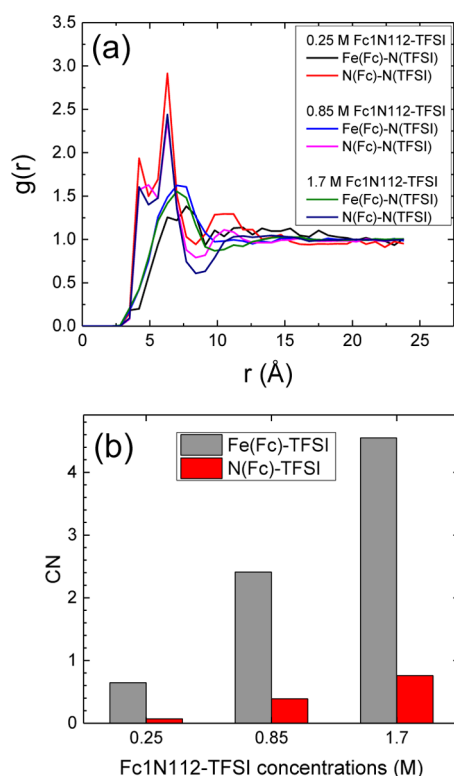


Figure 5. (a) Radial distribution function of the chain side of Fc1N112⁺ and the ring side of Fc1N112⁺ with the nitrogen atom of the TFSI anion at 0.25, 0.85, and 1.7 M at 323 K. The RDF shows a small peak (at ~4.5 Å) followed by higher intensity peak (at ~6.5 Å), indicating participation in either a first or second solvation shell. The broader peak of Fe(Fc)-N(TFSI) is due to steric hindrance as the Fe atom is confined between two cyclopentadienyl rings. (b) The coordination number (CN) of Fe-TFSI is much higher than N-TFSI at all concentrations, indicating preferential interactions of the TFSI[−] anion with the ring side of Fc1N112⁺ as compared to the ionic liquid chain side. Also, the CNs of Fe-TFSI and N-TFSI increase with increases in concentration, leading to formation of large aggregates at the solubility limit.

interactions with the ionic chain, showing a small peak (~4.5 Å) followed by a higher intensity peak (~6.5 Å) due to its participation in either the first or second solvation shell, respectively (see Figure 5a). The decrease in intensity of the first solvation peak with an increase in solute concentration indicates a preferential interaction of TFSI[−] with the cyclopentadienyl rings (TFSI-Fe) over the ionic chains (TFSI-N), which is in good agreement with the observed crystal structure of the Fc1N112⁺-TFSI[−] salt⁶ (see Figure S10). The CN of the TFSI[−] anion with ring and ionic chain sites of the Fc1N112⁺ cation over various solute concentrations are shown in Figure 5b. At a concentration of 0.25 M, the TFSI[−] anion has a very low CN around Fc1N112⁺ (<1), indicating a high probability for solvent separated ion pairs (i.e., the Fc1N112⁺ solvation shell is primarily occupied by solvent molecules). At higher concentrations (0.85 M), the CN significantly increases (~2), indicating that contact-ion pair formation is increasing, with the

possibility of agglomeration. At the solubility limit, Fc1N112⁺ has a very high CN (>4) for TFSI[−], indicating aggregate formation due to close packing of contact-ion pairs, where the anions are shared by more than one cation.²² In addition, the evolution of CN between Fc1N112⁺ cations to 3.1 at 1.7 M also reveals agglomeration with severe overlapping of their solvation spheres. These CN analyses clearly corroborate and validate the contact-ion pair formation and subsequent agglomeration revealed in ¹H NMR relaxation measurements, as well as recent studies of ¹³C, ¹⁷O, and ¹H chemical shifts utilizing both experiments and computations.²³ The slower reorientational motion and shorter distances between adjacent Fc1N112⁺ cations observed from relaxation measurements reflect and report on the significant cluster formation at higher solute concentrations.

CONCLUSIONS

The enhanced solubility of a polyatomic redox solute (Fc1N112-TFSI) within a ternary solvent mixture is predicted to be associated with highly selective solvation processes. At lower solute concentrations, the bulk solvent molecules compete to solvate preferential regions through active solvent exchange mechanisms. This solvation process has both solvent–solvent and ion–solvent components as dominant interactions with diminished ion–ion interactions. At higher concentrations, the solvent competition is drastically reduced due to the drop in available bulk solvent molecules and thereby enhances the ion–solvent type interaction through their preferential siting around Fc1N112⁺ cations. Simultaneously, increases in contact-ion pair formation reflect a porous solvation shell where Fc1N112⁺-TFSI[−] interaction probabilities are greatly enhanced. Near the solubility limit (~1.7 M), the overlapping solvation shells start to produce agglomeration of contact-ion pairs, initiating precipitate-like extended network formation. Overall, maintaining relatively strong ion–solvent interactions is critical for designing electrolytes with higher solute concentrations. It is clear that careful attention to the evolving and dynamic solvation structure in realistic electrolytes is needed to obtain the desired functional properties, which include viscosity and conductivity for novel battery systems such as nonaqueous redox flow batteries.⁵

ASSOCIATED CONTENT

Supporting Information

The Supporting Information is available free of charge on the ACS Publications website at DOI: 10.1021/acs.jpcc.6b09114.

Further information for T_1 analysis and MD simulations (PDF)

AUTHOR INFORMATION

Corresponding Authors

*E-mail: karl.mueller@pnnl.gov.

*E-mail: vijay@pnnl.gov.

ORCID

Karl T. Mueller: 0000-0001-9609-9516

Notes

The authors declare no competing financial interest.

ACKNOWLEDGMENTS

This research was led intellectually by researchers within the Joint Center for Energy Storage Research (JCESR), an Energy

Innovation Hub funded by the U.S. Department of Energy (DOE), Office of Science, Basic Energy Sciences (BES). The NMR measurements were performed at the Environmental Molecular Sciences Laboratory (EMSL), a national scientific user facility sponsored by the DOE's Office of Biological and Environmental Research and located at Pacific Northwest National Laboratory (PNNL). Work at LBNL was supported by the Department of Energy under Contract No. DE-AC02-06CH11357. We also thank the National Energy Research Scientific Computing Center (NERSC) for providing computing resources. The synthesis of Fc1N112-TFSI and the preparation of the electrolytes were supported by the U.S. DOE's Office of Electricity Delivery and Energy Reliability under Contract No. 57558. PNNL is operated for the U.S. DOE by Battelle Memorial Institute under contract number DE-AC05-76RL01830.

REFERENCES

- (1) Barnes, T. A.; Kaminski, J. W.; Borodin, O.; Miller, T. F. Ab Initio Characterization of the Electrochemical Stability and Solvation Properties of Condensed-Phase Ethylene Carbonate and Dimethyl Carbonate Mixtures. *J. Phys. Chem. C* **2015**, *119* (8), 3865–3880.
- (2) Xu, K. Electrolytes and Interphases in Li-Ion Batteries and Beyond. *Chem. Rev.* **2014**, *114* (23), 11503–11618.
- (3) Agmon, N. The Dynamics of Preferential Solvation. *J. Phys. Chem. A* **2002**, *106* (32), 7256–7260.
- (4) Ladanyi, B. M.; Maroncelli, M. Mechanisms of solvation dynamics of polyatomic solutes in polar and nondipolar solvents: A simulation study. *J. Chem. Phys.* **1998**, *109* (8), 3204–3221.
- (5) Wei, X.; Cosimbescu, L.; Xu, W.; Hu, J. Z.; Vijayakumar, M.; Feng, J.; Hu, M. Y.; Deng, X.; Xiao, J.; Liu, J.; Sprenkle, V.; Wang, W. Towards High-Performance Nonaqueous Redox Flow Electrolyte Via Ionic Modification of Active Species. *Adv. Energy Mater.* **2015**, *5* (1), 1400678.
- (6) Cosimbescu, L.; Wei, X.; Vijayakumar, M.; Xu, W.; Helm, M. L.; Burton, S. D.; Sorensen, C. M.; Liu, J.; Sprenkle, V.; Wang, W. Anion-Tunable Properties and Electrochemical Performance of Functionalized Ferrocene Compounds. *Sci. Rep.* **2015**, *5*, 14117.
- (7) Pronk, S.; Páll, S.; Schulz, R.; Larsson, P.; Bjelkmar, P.; Apostolov, R.; Shirts, M. R.; Smith, J. C.; Kasson, P. M.; van der Spoel, D.; et al. GROMACS 4.5: a high-throughput and highly parallel open source molecular simulation toolkit. *Bioinformatics* **2013**, *29* (7), 845–.
- (8) Martínez, L.; Andrade, R.; Birgin, E. G.; Martínez, J. M. Packmol: A package for building initial configurations for molecular dynamics simulations. *J. Comput. Chem.* **2009**, *30* (13), 2157–2164.
- (9) Bussi, G.; Donadio, D.; Parrinello, M. Canonical sampling through velocity rescaling. *J. Chem. Phys.* **2007**, *126* (1), 014101.
- (10) Han, K. S.; Rajput, N. N.; Wei, X.; Wang, W.; Hu, J. Z.; Persson, K. A.; Mueller, K. T. Diffusional motion of redox centers in carbonate electrolytes. *J. Chem. Phys.* **2014**, *141* (10), 104509.
- (11) Sudmeier, J. L.; Anderson, S. E.; Frye, J. S. Calculation of Nuclear Spin Relaxation Times. *Concepts Magn. Reson.* **1990**, *2* (4), 197–212.
- (12) Latanowicz, L.; Medycki, W.; Jakubas, R. Complex molecular dynamics of (CH₃NH₃)₅Bi₂Br₁₁ (MAPBB) protons from NMR relaxation and second moment of NMR spectrum. *J. Magn. Reson.* **2011**, *211* (2), 207–216.
- (13) Gutowsky, H. S.; Woessner, D. E. Nuclear Magnetic Spin-Lattice Relaxation in Liquids. *Phys. Rev.* **1956**, *104* (3), 843–844.
- (14) Bakhmutov, V. I. *Practical NMR Relaxation for Chemists*; John Wiley & Sons, Ltd: Chichester, U.K., 2004.
- (15) Hou, J.; Zhang, Z.; Madsen, L. A. Cation/Anion Associations in Ionic Liquids Modulated by Hydration and Ionic Medium. *J. Phys. Chem. B* **2011**, *115* (16), 4576–4582.
- (16) Levy, G. C. Carbon-13 spin-lattice relaxation. *Tetrahedron Lett.* **1972**, *13* (35), 3709–3712.
- (17) Takeuchi, M.; Matubayasi, N.; Kameda, Y.; Minofar, B.; Ishiguro, S.-i.; Umebayashi, Y. Free-Energy and Structural Analysis of Ion Solvation and Contact Ion-Pair Formation of Li⁺ with BF₄⁻ and PF₆⁻ in Water and Carbonate Solvents. *J. Phys. Chem. B* **2012**, *116* (22), 6476–6487.
- (18) Sun, Z.; Zhang, W.; Ji, M.; Hartsock, R.; Gaffney, K. J. Contact Ion Pair Formation between Hard Acids and Soft Bases in Aqueous Solutions Observed with 2DIR Spectroscopy. *J. Phys. Chem. B* **2013**, *117* (49), 15306–15312.
- (19) Erdemir, D.; Lee, A. Y.; Myerson, A. S. Nucleation of Crystals from Solution: Classical and Two-Step Models. *Acc. Chem. Res.* **2009**, *42* (5), 621–629.
- (20) Zimmermann, N. E. R.; Vorselaars, B.; Quigley, D.; Peters, B. Nucleation of NaCl from Aqueous Solution: Critical Sizes, Ion-Attachment Kinetics, and Rates. *J. Am. Chem. Soc.* **2015**, *137* (41), 13352–13361.
- (21) Thérien-Aubin, H.; Zhu, X. X.; Moorefield, C. N.; Kotta, K.; Newkome, G. R. Effect of Ionic Binding on the Self-Diffusion of Anionic Dendrimers and Hydrophilic Polymers in Aqueous Systems as Studied by Pulsed Gradient NMR Techniques. *Macromolecules* **2007**, *40* (10), 3644–3649.
- (22) Henderson, W. A. Glyme–Lithium Salt Phase Behavior. *J. Phys. Chem. B* **2006**, *110* (26), 13177–13183.
- (23) Deng, X.; Hu, M.; Wei, X.; Wang, W.; Mueller, K. T.; Chen, Z.; Hu, J. Z. Nuclear magnetic resonance studies of the solvation structures of a high-performance nonaqueous redox flow electrolyte. *J. Power Sources* **2016**, *308*, 172–179.